AD_____

GRANT NUMBER: DAMD17-94-J-4341

TITLE: The Tumor Suppressor Protein p53 and its Physiological Splicing Variant p53as in a Mouse Mammary Cancer Model

PRINCIPAL INVESTIGATOR: Dr. Molly Kulesz-Martin

CONTRACTING ORGANIZATION: Health Research, Inc., Roswell Division
Buffalo, New York 14263

REPORT DATE: October 1995

TYPE OF REPORT: Annual

PREPARED FOR: U.S. Army Medical Research and Materiel Command
Fort Detrick, Maryland 21702-5012

REPORT DOCUMENTATION PAGE

Form Approved
OMB No. 0704-0188

1. AGENCY USE ONLY *(Leave blank)*	2. REPORT DATE	3. REPORT TYPE AND DATES COVERED
	October 1995	Annual 1 Oct 94 - 30 Sep 95

4. TITLE AND SUBTITLE
The Tumor Suppressor Protein p53 and its Physiological Splicing Variant p53as in a Mouse Mammary Cancer Model

5. FUNDING NUMBERS
DAMD17-94-J-4341

6. AUTHOR(S)
Dr. Molly Kulesz-Martin

7. PERFORMING ORGANIZATION NAME(S) AND ADDRESS(ES)
Health Research, Inc., Roswell Division
Buffalo, New York 14263

8. PERFORMING ORGANIZATION REPORT NUMBER

9. SPONSORING/MONITORING AGENCY NAME(S) AND ADDRESS(ES)
U.S. Army Medical Research and Materiel Command
Fort Detrick, Maryland 21702-5012

10. SPONSORING/MONITORING AGENCY REPORT NUMBER

11. SUPPLEMENTARY NOTES

12a. DISTRIBUTION/AVAILABILITY STATEMENT
Approved for public release; distribution unlimited

12b. DISTRIBUTION CODE

13. ABSTRACT *(Maximum 200 words)*

The proposed studies seek to explore cellular and molecular aspects of p53 function that may contribute to the development and progression of breast cancer. The hypotheses are: 1) that p53 and a novel physiological splicing variant, p53as, have distinct stability in cells, distinct expression during the cell cycle, and distinct associated proteins; 2) that p53as has different specificity or affinity for DNA binding sequences than p53; and 3) that p53 and p53as mRNA and protein are differentially expressed in mouse mammary preneoplastic and neoplastic cells and tissues with implications for breast cancer detection, prognosis or treatment.

14. SUBJECT TERMS
tumor suppressor p53, mammary cancer, cell cycle, DNA binding, carcinogenesis, epidermal cells, breast cancer

15. NUMBER OF PAGES
50

16. PRICE CODE

17. SECURITY CLASSIFICATION OF REPORT	18. SECURITY CLASSIFICATION OF THIS PAGE	19. SECURITY CLASSIFICATION OF ABSTRACT	20. LIMITATION OF ABSTRACT
Unclassified	Unclassified	Unclassified	Unlimited

GENERAL INSTRUCTIONS FOR COMPLETING SF 298

The Report Documentation Page (RDP) is used in announcing and cataloging reports. It is important that this information be consistent with the rest of the report, particularly the cover and title page. Instructions for filling in each block of the form follow. It is important to ***stay within the lines*** to meet ***optical scanning requirements***.

Block 1. Agency Use Only *(Leave blank)*.

Block 2. Report Date. Full publication date including day, month, and year, if available (e.g. 1 Jan 88). Must cite at least the year.

Block 3. Type of Report and Dates Covered. State whether report is interim, final, etc. If applicable, enter inclusive report dates (e.g. 10 Jun 87 - 30 Jun 88).

Block 4. Title and Subtitle. A title is taken from the part of the report that provides the most meaningful and complete information. When a report is prepared in more than one volume, repeat the primary title, add volume number, and include subtitle for the specific volume. On classified documents enter the title classification in parentheses.

Block 5. Funding Numbers. To include contract and grant numbers; may include program element number(s), project number(s), task number(s), and work unit number(s). Use the following labels:

C	- Contract	PR	- Project
G	- Grant	TA	- Task
PE	- Program Element	WU	- Work Unit Accession No.

Block 6. Author(s). Name(s) of person(s) responsible for writing the report, performing the research, or credited with the content of the report. If editor or compiler, this should follow the name(s).

Block 7. Performing Organization Name(s) and Address(es). Self-explanatory.

Block 8. Performing Organization Report Number. Enter the unique alphanumeric report number(s) assigned by the organization performing the report.

Block 9. Sponsoring/Monitoring Agency Name(s) and Address(es). Self-explanatory.

Block 10. Sponsoring/Monitoring Agency Report Number. *(If known)*

Block 11. Supplementary Notes. Enter information not included elsewhere such as: Prepared in cooperation with...; Trans. of...; To be published in.... When a report is revised, include a statement whether the new report supersedes or supplements the older report.

Block 12a. Distribution/Availability Statement. Denotes public availability or limitations. Cite any availability to the public. Enter additional limitations or special markings in all capitals (e.g. NOFORN, REL, ITAR).

DOD	- See DoDD 5230.24, "Distribution Statements on Technical Documents."
DOE	- See authorities.
NASA	- See Handbook NHB 2200.2.
NTIS	- Leave blank.

Block 12b. Distribution Code.

DOD	- Leave blank.
DOE	- Enter DOE distribution categories from the Standard Distribution for Unclassified Scientific and Technical Reports.
NASA	- Leave blank.
NTIS	- Leave blank.

Block 13. Abstract. Include a brief *(Maximum 200 words)* factual summary of the most significant information contained in the report.

Block 14. Subject Terms. Keywords or phrases identifying major subjects in the report.

Block 15. Number of Pages. Enter the total number of pages.

Block 16. Price Code. Enter appropriate price code *(NTIS only)*.

Blocks 17. - 19. Security Classifications. Self-explanatory. Enter U.S. Security Classification in accordance with U.S. Security Regulations (i.e., UNCLASSIFIED). If form contains classified information, stamp classification on the top and bottom of the page.

Block 20. Limitation of Abstract. This block must be completed to assign a limitation to the abstract. Enter either UL (unlimited) or SAR (same as report). An entry in this block is necessary if the abstract is to be limited. If blank, the abstract is assumed to be unlimited.

*U.S.GPO:1993-0-358-779

FOREWORD

Opinions, interpretations, conclusions and recommendations are those of the author and are not necessarily endorsed by the US Army.

____ Where copyrighted material is quoted, permission has been obtained to use such material.

____ Where material from documents designated for limited distribution is quoted, permission has been obtained to use the material.

MLM Citations of commercial organizations and trade names in this report do not constitute an official Department of Army endorsement or approval of the products or services of these organizations.

____ In conducting research using animals, the investigator(s) adhered to the "Guide for the Care and Use of Laboratory Animals," prepared by the Committee on Care and Use of Laboratory Animals of the Institute of Laboratory Resources, National Research Council (NIH Publication No. 86-23, Revised 1985).

____ For the protection of human subjects, the investigator(s) adhered to policies of applicable Federal Law 45 CFR 46.

MLM In conducting research utilizing recombinant DNA technology, the investigator(s) adhered to current guidelines promulgated by the National Institutes of Health.

MLM In the conduct of research utilizing recombinant DNA, the investigator(s) adhered to the NIH Guidelines for Research Involving Recombinant DNA Molecules.

____ In the conduct of research involving hazardous organisms, the investigator(s) adhered to the CDC-NIH Guide for Biosafety in Microbiological and Biomedical Laboratories.

Molly Rules Martin 10-8-95

PI - Signature Date

TABLE OF CONTENTS

INTRODUCTION

Regulation of the cell cycle either by gene products needed for progression through the cell cycle or by gene products that act as checkpoints to monitor and stop progression is intrinsically related to oncogenesis. One gene product which monitors cell cycle progression is p53, a tumor suppressor which is deleted or mutated in more than 50% of all human cancers including breast adenocarcinomas. Normal functions of wild type p53 point to its role in cell cycle regulation and include the ability to arrest cells at the G1 phase of the cell cycle, to initiate apoptotic cell death, to aid in cell differentiation, and to be involved in the cellular response to DNA damage. The mechanism employed by p53 for all these functions may result from its capacity to affect transcription, both as an activator for some genes and as a repressor for others (for a review of p53 functions see Haffner and Oren, 1995).

This laboratory has observed a wild type alternatively spliced form of p53, designated p53as, in normal and malignant mouse cells and tissues which is expressed at approximately 25-30% of the major p53 form (Han et al., 1990; Han et al.,1992). The alternative splicing of p53as mRNA results in a substitution of 17 different amino acids at the carboxyl terminus and shortens the p53as protein by 9 amino acids when compared with p53 protein. p53as expression is localized to the nucleus and is preferentially found in cells in the G2 phase of the cell cycle (Kulesz-Martin et al., 1994). This is unlike the expression of the regular

form of p53 which is primarily found in cells in G1. These observations advocate a distinct role for p53as in cell cycle regulation.

Electrophoretic mobility shift assays indicate that p53as protein binds sequence-specific DNA more efficiently than p53 and needs no activation to do so as does p53 (Wu et al., 1994). Bayle et al. (1995) have suggested that p53as has lost the ability to bind nucleic acids in a nonspecific manner. These data imply a potential mechanism for regulating p53 functions by increasing or decreasing the ratio of p53as:p53 present in cells.

In vitro translated p53as protein forms homo-tetramers and also forms hetero-tetramers when co-translated with p53 (Wu et al., 1994). Thus, interaction between the two endogenous forms of the wild type p53 proteins that could play a role in the functions attributed to p53.

This project was undertaken to begin an examination of the distinct cellular and molecular aspects of p53 and p53as functions that may influence the development and progression of cancer. In view of the prominence of p53 mutations in breast disease and cancer, understanding the functional roles of p53 and p53as in normal and malignant cells should be of paramount importance. We proposed to examine these aspects during early changes from normal to preneoplastic and malignant stages in a breast cancer model (Medina et al., 1993a, 1993b) and in a mouse epidermal model developed in this laboratory.

A mouse mammary epithelial cell line recently developed by Medina et al. (1993a) can be transplanted into syngenic mouse fat pads to give rise to mammary preneoplastic outgrowths. These in vivo outgrowths,

designated TM (for "tumor mammary"), have tumor-producing capabilities and include lines which respond to estrogen. Cell lines derived from the TM outgrowth lines have been established (Medina et al., 1993b).

TM outgrowths have been examined for the expression of p53 using the polyclonal CM-5 antibody which would be expected to bind both p53 and p53as at multiple epitopes. Overexpression of p53 was observed in the TM neoplastic outgrowths with the exception of TM9 (Medina, unpublished data).

A murine clonal epithelial cell lineage in which normal, initiated, benign, and malignant stages are represented has been developed in this laboratory. Like the mammary model, cell types have been established at various stages of preneoplasia and malignancy. In addition, the derivation of these different stages in the epidermal model from the same cloned parental cell offers controls for proliferative and differentiative states within the same genetic lineage.

During this first year we proposed to: **1**) determine p53 and p53as expression in preneoplastic and neoplastic mouse mammary cell lines and tissues by immunofluorescence and immunohistochemistry (Task 1), **2**) quantitate p53 and p53as mRNA in preneoplastic and neoplastic mouse mammary cell lines and tissues using reverse transcription and polymerase chain reaction amplification (Task 1), **3**) purify p53 and p53as proteins from a baculovirus system (Task 2), and **4**) determine the oligomerization properties of p53as with p53 using FPLC and immunoblotting and proteins produced by in vitro translation or purified

from a baculovirus system (Task 3). In addition, we planned to work out the conditions for centrifugal elutriation to isolate cells at different stages of the cell cycle in sufficient quantity for half-life studies which would be carried out in the second year of this proposal.

In the subsequent years of this grant we proposed to perform half-life studies of p53 and p53as throughout the cell cycle in mouse mammary cells that have been fractionated by means of centrifugal elutriation and in synchronized mouse epidermal cells (Task 4). Potential p53as DNA binding sites will be determined by binding DNA to p53as protein, immunoprecipitating with specific antibody, and sequencing bound DNA fragments (Task 5). We will seek p53- and p53as-associated proteins which may affect protein stability using coimmunoprecipitation or affinity chromatography with baculovirus-produced p53 or p53as. Initial steps to determine the identity of these associated proteins will include comparison with known p53-associated proteins of similar molecular weight or novel putative p53as-associated proteins in the database, and preparation of coimmunoprecipitated proteins for partial amino acid sequencing (Task 6).

RESULTS AND METHODS

Task 1 (Aim 1). Determination of p53 and p53as expression in the mouse mammary model: Immunoreactivity in preneoplastic and neoplastic cell lines.

Our initial choices of TM lines included TM3, TM12, and TM4 which progressed from hyperplasia and zero tumor incidence on reimplantation (TM3) to neoplasia with low tumor incidence (TM12) and neoplasia with high tumor incidence (TM4). We also examined TM9 and TM10 both of which were neoplastic with low tumor incidence. The TM12 cell line was composed of two morphological cell types: a slow growing rounded cell type which grew in circumscribed areas which were designated "island" cells, and a fast growing fibroblastic type cell that grew between the islands and which were designated "spaces" cells. These two TM12 cell morphologies were separated and examined in the isolated state and when grown together.

Immunofluorescence assays were carried out on cells that were plated at 5 X 10^4 cells/3.2 cm^2 in 0.2 ml on cleaned coverslips. The cells were incubated at 37°C with 5% CO_2 for 2-4 hours to allow for attachment. Three ml of growth medium/60 mm dish was added and cells were incubated until 50% confluent, usually one day. Cells were treated with Actinomycin D, gentamycin, or X-ray or left untreated at this time. Treatment continued for 48 hours except for TM10 cells which were treated for an additional 24 hours. Cells were then fixed by washing twice with PBS and immersing in 3 ml cold 100% ethanol for 30 min.

Table 1 shows the reactivities of the panel of antibodies that were used in the immunofluorescence studies. To stain cells, ethanol was removed from the cells on coverslips and replaced with PAB (PBS/0.5% BSA/0.1% sodium azide). Cells were allowed to rehydrate for 10 min. at

room temperature before blocking with 25 µl of 5% normal goat serum per coverslip. This was incubated for 1 hour at room temperature, the blocking mixture removed and replaced with 25 µl of the primary antibody. Final concentrations of each antibody were: 7-10 µg/ml affinity-purified rabbit anti-p53as or 10 µg/ml of PAb421, 240, or 246. Dishes were covered in plastic wrap and incubated humidified at 4°C overnight. After washing twice in 3 ml PAB for 15 min, 25 µl of the secondary antibody (1:300 dilution of Texas Red-conjugated goat anti-rabbit immunoglobulin (Southern Biotechnology Associates, Inc.) or of FITC-conjugated goat anti-mouse (Southern Biotechnology Associates, Inc.)) was added. This was incubated for 30 min at room temperature in darkness before washing. Coverslips were mounted using aqueous mountant on a microscope slide by placing them cell side down. Slips were allowed to settle on a flat surface for at least 1 hour.

Figure 1 shows the results of these immunofluorescence experiments with TM3 and TM10, and Table 2 summarizes these results from all the examined TM cell lines. TM3 and TM4 were positive for the polyclonal antibody specific for p53as (ApAs) and PAb421 and 240 while negative for PAb246 revealing that although TM3 and TM4 lines contained p53 and p53as, it was a mutated form of the protein. TM12 island and TM12 spaces cells expressed little and no p53as, respectively. PAb421 reactivity was low in the total TM12 population and in the island cells, but was expressed in 40% of the TM12 spaces cells, Reactivity to

PAb246 was noted in these three cell populations and they were all negative for PAb240. Although these cells contain wild type p53, they have very low amounts of p53as. Fifty percent of TM9 cells were positive for PAb421, however they also showed reactivity to PAb240 and little reactivity to PAb246 indicating a mutated form of p53. In addition, TM9 had very little ApAs reactivity. TM10 had very low amounts of p53 and p53as in untreated, actinomycin D treated, and X-ray treated cells. However, 60 nM genistein treatment for 3 days elevated the amount of ApAs reactivity in these cells.

Task 1 (Aim 1). Determination of p53 and p53as expression in the mouse mammary model: mRNA by reverse transcription and PCR or quantitation by RNase protection assay.

TM3, TM4, and TM12 cells were grown in 150 mm tissue culture plates to approximately 80% confluency at which time the medium was aspirated, the cells washed once in PBS, and scraped in 3 ml Ultraspec™ RNA solution (Biotecx Laboratories, Inc.). Total RNA isolation was carried out following the procedure of the manufacturer. The RNA pellet was dissolved in diethyl pyrocarbonate (DEPC)-treated H_2O and RNasin (Promega). Fifteen µl reverse transcription (RT) assays were carried out using 1 µg of total RNA in buffer (10 mM Tris pH 8.3/20 mM KCl/3,5 mM $MgCl_2$/100 µM dNTPs/10 units of RNasin) containing 1.1 µg of random hexamer and 30 units of AMV-reverse transcriptase (Promega) for 30 min at 44°C. Two µl of the RT reaction were used in a 20 µl PCR

reaction containing 10 mM Tris pH 8.8, 3.5 mM $MgCl_2$, 25 mM KCl, 150 μM dNTPs, 2 μM of each PCR primer, and 1 unit of Taq DNA polymerase (Boehringer Mannheim). Thirty PCR cycles were carried out by denaturation for 1 min at 94°C, annealing for 1 min at 65°C, and elongation for 2 min at 72°C. The RS4 primers used for PCR have been previously described (Han, 1992). Initial experiments comparing RT-PCR assays using total RNA and polyA$^+$ RNA (FastTrack mRNA Isolation System, Invitrogen) indicated no advantage to using polyA$^+$ RNA (data not shown), thus all subsequent experiments used total RNA.

Figure 2 shows the data from RT-PCR reactions using total RNA isolated from TM3, TM4, and TM12, TM12 islands, and TM12 spaces cells. All contained the 517 bp product from p53 mRNA and the 613 bp product from the alternatively spliced message.

Task 2 (Aim 2, 3). Production and purification of p53as and p53 proteins in the baculovirus system: a. p53 and p53as cDNA construction into the insect virus vector.

Two p53-containing constructions were made, one in the pVL1393 vector and one in the pBlueBacIII vector by ligating a BglII-BamHI DNA fragment containing p53 cDNA into the BamHI site of the vector. To generate p53as in pVL1393, the carboxy terminus from an internal StuI site to the regenerated BamHI site was replaced with a similar PCR fragment containing the carboxy terminus of p53as. This construction was sequenced to verify it contained the wild type p53as sequence (data not shown).

Task 2 (Aim 2, 3). Production and purification of p53as and p53 proteins in the baculovirus system: b. insect cell clones containing recombinant virus selected; recombinant virus cloned.

Sf9 insect cells were grown in Grace's antheraea insect media (Invitrogen) with 10% fetal calf serum (ICN Flow), 0.1% pluronic F-68 (JRH Scientific), and 50 µg/ml gentamycin sulfate (Sigma) at 27°C. Transfection of p53 or p53as-containing plasmid DNA was accomplished according to directions supplied in the BaculoGold™ Transfection Kit (PharMingen). A single plaque was picked and a low titer virus suspension made as detailed in the Invitrogen manual entitled "A Manual of Methods for Baculovirus Vectors and Insect Cell Culture Procedures" by Max D. Summers and Gale E. Smith. Recombinant viral DNA containing p53-pVL1393, p53-pBlueBacII or p53as-pVL1393 DNA was isolated and subjected to PCR analysis to verify the presence of insert DNA (data not shown). Infected insect cells were analyzed using ELISA with ApAs or PAb421 antibodies to confirm the presence of p53 or p53as proteins. Production of p53as protein was verified (data not shown), however infected cells containing p53-pVL1393 or p53-pBlueBacIII DNA did not produce p53 protein even though the viruses did contain p53 DNA. This result was repeated on subsequent transfections with p53-pVL1393 and p53-pBlueBacII DNA. Therefore we obtained low titer p53-containing virus as a gift from Dr. Carol Prives.

The p53 low titer virus suspension from Dr. Prives has been subjected to four consecutive rounds of virus amplification (MOI=1)

reaching a titer of 1 X 10^7 pfu/ml. Another round of amplification will be necessary for optimum p53 production.

Recombinant p53as virus was subjected to four consecutive rounds of Sf9 infection using a multiplicity of infection (MOI) of 1, to amplify the titer to 1 X 10^8 pfu/ml.

Task 2 (Aim 2, 3). Production and purification of p53as and p53 proteins in the baculovirus system: c. Insect cells producing protein grown, lysed, and p53as or p53 protein purified using PAb421 or ApAs affinity columns.

p53as protein was produced in Sf9 cells using a MOI of 5 following instructions from PharMingen to determine if the protein was secreted into the medium. Cells were lysed in 10 mM Tris pH 7.5/150 mM NaCl/1 mM EDTA/0.5 mM DTT/0.1% NP-40/1 mM PMSF/7 μM leupeptin/1.8 μg/ml pepstatin. Cell lysates and medium were subjected to electrophoresis and western immunoblotting using ApAs antibody. The majority of p53as was located in the cell lysate and not in the medium (data not shown).

A time course of p53as protein production after infection of Sf9 cells was carried out to optimize protein production. Thirty-five ml of Sf9 cells were infected at a MOI=5 and 5 ml samples taken at this time and 1-5 days post infection. A western blot using polyclonal antibody CM5 indicated that two days post infection was the optimum time for maximum protein production (Figure 3). This was in agreement with independent experiments in this laboratory showing that human p53

protein production in Sf9 cells also was optimum two days post infection (data not shown). The regular form of murine p53 will be tested in the same way as soon as the high titer virus is prepared.

A PAb421 affinity column for purification of p53 was prepared following the protocol from the manufacturer using 1 ml of BioRad Affi-Gel Hz and 420 μg of PAb421 (Oncogene Science). This matrix covalently binds to the immunoglobulin carbohydrates. The affinity matrix was tested for its binding efficiency by batch adsorbing an available lysate from 100 ml of human p53-infected Sf9 cells for 2 hours at 4°C with gentle rocking, batch washing the matrix with1 column volume of 100 mM Tris pH 8.0/150 mM NaCl/0.5 mM EDTA, and batch eluting p53 with 1 column volume twice of 0.1 M glycine pH 2.8/0.15 M NaCl. Figure 4 and 5 show the profile of this batch chromatography. While there is loss of contaminating proteins throughout the purification as seen in the Coomassie stained gel (Figure 4), much of p53 is not adsorbing to the column, allowing a major portion of the protein to flow through as shown in the western blot (Figure 5). This may reflect an overloading of the column and/or a need to adsorb the lysate for a longer time, both of which we will investigate.

A larger immunoaffinity column that could be used to purify both p53 and p53as was made using 2 mg of Pab242, whose epitope is amino acids 9-25, coupled to 2 ml of BioRad Affi-Gel Hz matrix as above. Calculations following covalent binding of the antibody indicated that ≥88% of the antibody had been coupled to the matrix. The lysate from a 50 ml p53as-infected Sf9 cell culture was batch-adsorbed to this matrix

overnight with gentle rocking at 4°C. The flow through was collected and the matrix washed three times with 1 column volume of PBS/0.5 M NaCl followed by another column volume wash of PBS/0.15 M NaCl. The p53 was eluted with 2 column volumes of 0.1 M glycine pH 2.8 and the two fractions were combined and concentrated by means of a Centricon filter. Figures 6 and 7 again show a loss of contaminating proteins throughout the purification shown on the Coomassie stained gel (Figure 6), but by western blot analysis (Figure 7), most of the p53as protein is not adsorbing to the matrix resulting in a poor yield of purified p53as. For example, in one affinity column experiment 64 mg of total protein from a cellular lysate yielded 96 μg of purified p53as, with most of this protein not being retained by the antibody column. One possible reason for poor adsorption is that the linkage of the antibody to the matrix is in some way interfering with the antibody binding of p53 and p53as. We will address this hypothesis by using a different matrix, protein A sepharose, which covalently binds specifically to two constant regions in the heavy chain of the antibody.

Task 3 (Aims 2,3). Determination of oligomerization properties of p53as with p53; a. FPLC fractionation of monomers, dimers, and tetramers of p53as alone or in combination with p53 protein produced in vitro (reticulocyte lysates) and in the baculovirus system (homo- and hetero-oligomerization); detection of p53 or p53as protein forms in each fraction either by immunoprecipitation followed by immunoblotting or by solid-phase immunoassay using monoclonal anti-p53 coated on ELISA wells to

capture oligomers and the rabbit polyclonal to specifically detect p53as forms.

In vitro translation of p53 and p53as was carried out using a rabbit reticulocyte lysate (Promega) and the proteins were fractionated by gel filtration on a Superose 6 column (Pharmacia) as previously described (Wu, 1994). Figure 8 shows the FPLC analysis and indicates that p53, p53as, and cotranslated proteins have the same elution profile, indicating primarily tetrameric forms in solution, as expected from the known properties of p53 protein. Electrophoretic mobility shift assays also indicate that p53as is capable of oligomerization, not only with itself, but also with p53 (Wu et al., 1994). Thus, p53as protein has the ability to form dimers and tetramers.

Task 4 (Aim 2). Determination of half-life of ^{35}S-labeled p53as and p53 proteins, immunoprecipitated and analyzed by electrophoresis. a. preneoplastic and neoplastic mouse mammary cell lines; b. cell cycle dependence in synchronized mouse fibroblasts; c. cell cycle dependence in mammary cells by centrifugal elutriation; verification of DNA content by flow cytometry. This task had been placed in the second year in our Statement of Work, but working conditions of centrifugal elutriation, cell synchronization, and protein half life determinations were needed as a prerequisite to these studies.

Centrifugal Elutriation

A Beckman J-6M centrifuge equipped with one standard elutriation chamber (rotor code 5.2) was used for centrifugal elutriation. If cells

were to be re-cultured after separation, the chamber and lines were sterilized with 200 ml undiluted bleach followed by 200 ml of 70% ethanol and 1-2 liters of sterile distilled water. The centrifuge temperature was maintained at 4°C throughout the run and bubbles cleared from the lines and chamber before use.

TM3 or TM4 cells were plated at 2 X 10^6/150 mm plate and allowed to grow until approximately 65-75% confluent. Cells were dissociated with 0.25% trypsin and 0.2% EDTA and resuspended in RPMI 1640 medium with 5% fetal calf serum and 1-3 μg/ml DNaseI. Fifty to 100 ml volumes were used to load the elutriation chamber. The pump speed was set at 500 rpm to give an elutriation rate of 10 ml/min. After cells were loaded at a centrifuge speed of 2200, the centrifuge speed was reduced to 1500 rpm and a 100 ml fraction collected. Rotor speed was decreased by increments of 100 rpm after collection of each 100 ml fraction while pump speed was maintained at a constant setting of 500 rpm. Ten 100 ml fractions were collected.

The fractions were centrifuged to pellet the cells and the pellet washed two times with MEM without serum. After the final wash, a small amount of residual MEM was used to resuspend the cells, and the resuspended cells were fixed in 100% ethanol at a density of ≤5 X 10^6 cells/ml. An aliquot of ethanol-fixed cells (1-2 X 10^6 cells) was centrifuged and resuspended in 300-400 μl PAB (PBS with 1% BSA and 0.1% sodium azide) and 2 μg/ml Hoechst dye was added ≥1 hour prior to flow cytometric analysis.

Flow cytometry was performed on a FACSTAR$^+$ dual 5W argon laser system (Becton Dickinson Immunocytometry Systems) as described (Kulesz-Martin, 1994).

Figure 9 is representative of flow cytometry data obtained from fixed TM3 cells after centrifugal elutriation. Placement of G1 and G2 cell cycle stages on the x-axis was determined by using mouse spleen cells as an external control. Cell cycle separation was best for G1 phase as shown in fraction 1 or 2 where the percentages of G1 cells were 89% and 85% respectively. Enrichment for S phase cells first appeared in fraction 3 where 78% cells were in G1 and 15% in S phase. Fraction 4 cells were 67% G1, 21% S, and 9% G2; fraction 5 was 48% G1, 30% S, and 18% G2; fraction 6 cells were 25% G1, 34% S, and 37% G2.

Two ways to improve yield and purity of discrete cell cycle phases were attempted, centrifugal elutriation followed by fluorescence activated cell sorting and synchronization (see below). In the first approach, cells were subjected to centrifugal elutriation to enrich for a particular cell cycle phase, followed by cell sorting to further separate one specific population from the enriched cells. The sorted cell population would be used for isolation of RNA and proteins. To keep the cells alive for RNA and protein isolation after cell sorting, Hoechst staining was done on live cells. To do this, fractionated cells were resuspended in RPMI 1640 plus 5% fetal calf serum at 1 X 10^6 cells/ml. CO_2 gas was bubbled through the culture medium to adjust the pH to 7.0 and Hoechst dye was added at 2 μg/ml. Cells were agitated at 37°C for 30 min,

centrifuged, resuspended in media plus 2 μg/ml Hoechst dye at a density of 5-10 X 10^6/ml, and kept on ice until sorting.

Since the amount of time between elutriation and RNA and protein isolation had to be minimized so that cells would not move out of the cell cycle phase in which they were isolated, the elutriated cells were not examined by flow cytometry to determine the fractions to be sorted, but fractions were combined based on previous experiments and then stained for cell sorting. Figure 10 is the centrifugal elutriation histogram profile of live TM4 cells that were used for sorting. Based on previous data with fixed TM4 cells, fractions 4-6 were combined to sort for G1 and S, while fractions 7-10 were combined to sort for S and G2. This was the first time that Hoechst staining was used on live cells and the data indicated a different elutriation profile than what was seen using fixed TM4 cells (data not shown) and TM3 cells (Figure 9). However, good isolation of G2 cells was obtained in combined fractions 4 through 6 where 62% of the cells were in G2 with centrifugal elutriation alone (Figure 10). Thus it appears that good separation of G1 cells and G2 cells is possible using this technique but not reproducible in all experiments. Although placement of G1 and G2 cell cycle stages on the x-axis was determined by using mouse spleen cells as an external control, occasionally misalignment of a histogram occured as is seen in the first fraction .

In spite of the less than optimal separation, RNA and protein lysates were made from the elutriated fractions of one run using TM4 cells for RT-PCR and western blot analyses. Figure 11 suggested that both p53 and p53as mRNAs were present in all fractions. Although RT-

PCR analysis is not quantitative, these initial results indicated very similar amounts of mRNA of both species in all fractions. Figure 12 shows similar amounts of p53 protein present in all elutriated fractions on a western immunoblot using PAb421.

Cell Synchronization

As an alternative means to select cell cycle stages, cell synchronization using serum starvation to arrest cells in G1 was done. Initially a protocol was used incorporating 5μg/ml aphidicolin with serum starvation (0.5%) for 24 hours, adding ^{3}H-thymidine to measure DNA synthesis in TM3 cells at various time points after removing the drug and adding back serum. However, the cells showed very poor uptake of ^{3}H-thymidine, <2000 cpm at the peak of incorporation (data not shown). Subsequent experiments with TM3 and TM10 mouse mammary cell lines and 291 and 291.05RAT mouse epidermal cell lines were carried out to examine various parameters in the procedure: 1) 0% or 0.2% serum during the starvation period was observed. 2) 2 or 8% serum for the mammary cell lines and 10 or 20% serum for the epidermal cell lines were examined after starvation times (normal growth medium for these cells lines are 2 and 10%, respectively), 3) serum starvation times of 15, 24, or 48 hours were observed, and 4) cell densities in12-well plates of 2.5×10^{4}, 4×10^{4}, or 5×10^{4}/well were examined. The best parameters for this experiment using TM3 cells were plating cells at 5×10^{4}/well in a 12-well plate and growing the cells for 48 hours. Serum starvation in 0.2% serum for 48 hours and restimulation of growth using medium with 2% serum. Optimum condition for 291 and 291.05RAT cells were plating

at 3.5 X 10^4 cells/well in a 12-well plate, growing for 48 hours, serum starvation in 0.2% serum for 48 hours, and restimulation in 10% serum. For all cell lines used, at various time points 1 μCi of ^{3}H-thymidine (Amersham, 85 Ci/mmol) was added to each well and the cells incubated for 1 hour at 37 °C in humidified CO_2. The cells were washed once in 1 ml PBS, 1 ml of 10% TCA was added to each well, and the plates were incubated at room temperature for 5 min. Each well was then washed twice with 1 ml PBS, 500 μl of 1 N NaOH was added to each well and the plates gently agitated at room temperature for 30 min. One hundred μl from each well was added to a scintillation vial containing 100 μl 1N HCl and 300 μl of H_20. After addition of 4.5 ml of scintillation fluid, the vials were vigorously vortexed and counted in a scintillation counter. All ^{3}H-thymidine uptake time points were done in triplicate.

Figure 13 shows an experiment with 291 and 291.05RAT cells plated at 3.5 X 10^4 cells/well. Both cell lines efficiently growth arrested after a 48 hour serum starvation and began to resume DNA synthesis approximately 8 hours post serum addition. The cells continued to incorporated ^{3}H-thymidine up to approximately 56 hours post serum addition at which time incorporation began to decrease.

These data indicate cell synchronization due to serum starvation will be a good way to investigate protein stability of p53 and p53as throughout the cell cycle, allowing a large amount of cells to be examined in G1, S, and G2 phases.

Protein Half-Life

Protein half-life studies were begun using proliferating TM3 and TM4 cells. Cells were grown to 70-80% confluency, washed twice in RPMI 1640 medium minus methionine containing 5% dialyzed fetal calf serum, and incubated at 37°C for 30 min in 10 ml/150 mm plate of the same (minus methionine) medium. This medium was replaced with 6 ml of the same medium containing 1.2 mCi ^{35}S-methionine (Amersham, 10 mCi/mmol) and the cells were incubated 1 hour at 37°C. At this time, the medium was removed, the plates washed once in 10 ml chase medium (RPMI 1640, 5% fetal calf serum, 15 µg/ml methionine), and 10 ml of the same medium added.

Plates were incubated for various chase times (each time point consisted of cells from 1-150 mm plate) then cells were washed in 10 ml PBS, scraped in 10 ml PBS, and the cell pellets washed once in PBS before lysing the cells in 100-200 µl lysis buffer (50 mM Tris pH 8.0, 150 mM NaCl, 1% NP-40, 1 mM PMSF, 5 mM leupeptin, 10 µg/ml pepstatin A) for ≥1 hour at 4°C. Lysate was cleared by centrifugation at 10,000 rpm (Sorvall SS34 rotor) for 30 min, the supernatant was removed and precleared for immunoprecipitations by adding 5 µl Protein G$^+$ and A agarose (Oncogene Science) and gently rocking for 1.5 hours at 4°C.

Immunoprecipitations were set up with either equal TCA-precipitable counts or equal amounts of protein (20-50 µg) plus 2 µg of ApAs or PAb421 antibody. Lysis buffer including protease inhibitors was used to achieve a final volume of 450 µl and the mixture rocked overnight at 4°C. Horseradish peroxidase-conjugated Protein A (Amersham) was then added to the ApAs reaction or goat-α-mouse IgG

(1:20,000) (Pierce) to the PAb421 reaction and the mixtures were rocked for 2 hours at 4°C. Immune complexes were precipitated by centrifugation for 1 minute, washed three times in lysis buffer containing protease inhibitors, and resuspended in 25 µl of 1X Laemmli loading buffer. After heating at 95°C for 5 minutes, the complexes were electrophoresed on a 7.5% polyacrylamide gel.

Figures 14 A and B shows an autoradiograph of immunoprecipitations using equal TCA-precipitable counts from proliferating TM3 cells. Densitometric scanning was performed on this autoradiograph and those data plotted on the graph shown in Figure 15. These data indicate a shorter half-life for p53 protein (approximately 5 hours) compared with p53as protein (approximately 6 hours). The half life of wild type p53 has been shown to be less than 30 minutes (Reich and Levine, 1984), however, mutated p53 has a longer half life (Reich, et al., 1983). The relatively long half life shown for p53 and p53as in TM3 and TM4 are indicative of a mutated p53/p53as which we also showed with immunofluorescence.

Half-life studies in proliferating TM4 cells were carried out and the immunoprecipitations made with equal protein amounts as shown in Figures 16 A and B. Figure 17 contains the relative density of these signals on the autoradiograph. As in TM4, the half life of p53 protein is shorter (approximately 5 hours) than the half life of p53as protein (approximately 6 hours). As with TM3, the longer half life of both proteins relative to p53 in normal cells is consistent with a mutated form as shown using immunofluorescence.

CONCLUSIONS

Task 1. The requirements for our study to compare p53 and p53as protein stability and cell cycle dependence are that mammary cells, nontumorigenic, premalignant, and highly tumorigenic with intermediate stages, are available. The mammary line TM3 selected as nontumorigenic was found to be unstable, converting to malignancy with passage (D. Medina, unpublished data) and contained a mutated p53 gene (the current study). Therefore other candidate lines (TM9 and TM10) were tested. TM9 was found to contain mutated p53 and TM10, like our original choice as an intermediate cell type TM12, contained very low levels of p53as. The half-life studies of mammary cell lines therefore will be amended to take advantage of the capacity of TM10 cells to elevate p53as levels in response to the DNA-damaging agent, genistein. This protocol offers advantages of 1) permitting determination of cell cycle dependence and comparative stability of the p53 and p53as forms, which is the original objective of Task 4, and 2) addressing an important functional property of p53 protein, its role in regulation of cell response to DNA damage. We have recently also determined that genistein treatment of TM10 cells increases the amount of p53as so as to be detectable by immunoprecipitation.

As originally proposed, we will continue these studies in a murine clonal epithelial cell lineage in which normal, initiated, benign, and malignant stages are represented while we continue to investigate the TM3 (high passage) and TM10 lines as representative of high- and low-

tumorigenic states, respectively. The mouse keratinocyte model system and the mouse mammary tumor system have similarities in that they include preneoplastic and malignant stages which exhibit decreased dependence upon EGF and other growth factors, form benign then malignant tumors when grafted to the site of origin in vivo, and have the ability to differentiate. Most important to this study, the epidermal cells contain a wild type p53 gene, are stable in phenotype and respond well to synchronization protocols. They offer a standard of comparison and means of protocol optimization which will be applied to the studies of mammary cells.

In addressing Task 1, we determined the expression of p53 and p53as in 5 TM cell lines including two morphologies from one line. Now that we have selected the TM cell lines and conditions to use for this study, we will complete Task 1 by carrying out immunohistochemistry of TM3 and TM10 and performing RT-PCR of TM10 RNA. This task should be finished within two months.

Task 2. Purification of p53 and p53as using the baculovirus system has progressed to the point where small amounts of pure (by Coomassie staining) p53as are available. We will make an antibody affinity column using Protein A sepharose to determine if that will improve the adsorption of the p53 to the column. One more round of virus amplification should be sufficient to obtain the titer needed for infection of insect cells for p53 protein production. This task should be finished within two months.

Task 3. Oligomerization studies of p53as and p53 in vitro translated proteins have demonstrated the presence of dimers and tetramers for both. This task has been completed.

Task 4. Centrifugal elutriation of TM3 and TM4 cells indicated that this method is useful for obtaining G1 phase cells, but is less suitable for separation of S or G2 phase cells. Centrifugal elutriation followed by cell sorting did not permit the separation of S and G2 cells in a suitable quantity for half life studies and has the disadvantage of prolonging cells in the suspended state, which could be detrimental for normal cycling. However, cell synchronization was achieved by serum starvation allowing the examination of the necessary high numbers of cells in half-life studies of p53 and p53as proteins throughout the cell cycle. We plan to continue to monitor the cell cycle phase by ^{3}H-thymidine uptake during the half-life studies.

The procedure for ^{35}S-methionine labeling of proteins and half-life studies has been worked out to achieve amounts of p53 and p53as proteins by immunoprecipitation easily visualized by autoradiography.

During this year we have laid the groundwork that will enable us to characterize the stability, conformation, association with other proteins, and sequence-specific DNA binding activity of p53as and p53 in a model system that encompasses the progression of cells from normal to preneoplastic and malignant stages of cancer. Future work will continue to investigate cellular and molecular features of p53 and p53as which may influence the development and progression of cancer and which

may lead to applications in diagnosis, prognosis, or treatment of breast cancers.

FIRST YEAR PROGRESS SUMMARY

Major points of progress made during the first year:

1. Mammary lines have been shown to express p53as both at the RNA level by RT-PCR and the protein level by immunoblotting.

2. p53as is an efficient, active DNA binding form in cells.

3. p53as has been shown to form tetramers in solution like p53, verifying its oligomerization. In addition, p53as has been demonstrated to form hetero-oligos with p53 increasing the possibilities for regulation of p53 functions by differences in the ratio of the two forms in cells.

4. Methods have been developed to select cell populations in distinct cell cycle stages and include centrifugal elutriation (G0/G1 distinct from G2/M) and cell synchronization (S distinct from G0/G1 and from G2/M. While the extent of these separations varied from experiment to experiment, continued monitoring during the course of the p53 and p53as half life studies should permit these experiments to be carried out appropriately.

5. Preliminary half life studies suggest that there are differences in the stability of p53as and p53 proteins. These differences will be measured during the second year of this study.

BIBLIOGRAPHY

Bayle, J.H., Elenbaas, B., and Levine, A.J. 1995. The carboxyl-terminal domain of the p53 protein regulates sequence-specific DNA binding through its nonspecific nucleic acid-binding activity. Proc. Natl. Acad. Sci. USA 92:5729-5733.

Haffner, R. and Oren, M. 1995. Biochemical properties and biological effects of p53. Curr. Opinion in Gen. and Dev. 5:84-90.

Han, K-A., Rothberg, P., Kulesz-Martin, M.F. 1990. Altered expression of wild type p53 tumor suppressor gene during murine epithelial cell transformation. Cancer Res 52:749-753.

Han, K-A., Kulesz-Martin, M.F. 1992. Alternatively spliced p53 RNA in transformed and normal cells of different tissue types. Nuc. Acids Res. 20:1979-1981.

Kulesz-Martin, M., Yoshida, M., Prestine, L., Uuspa, S. H., Bertram, J. S. 1985. Mouse cell clones for improved quantitation of carcinogen-induced altered differentiation. Carcinogenesis 6:1245-1254.

Kulesz-Martin, M., Blumenson, L., Manly, K.F., Siracky, J., and East, C. J. 1991. Tumor progression of murine epidermal cells after treatment in vitro with 12-O-tetradecanoylphorbol-132-acetate or retinoic acid. Cancer Res. 51:4701-4706.

Kulesz-Martin, M.F., Lisafeld, B., Huang, H., Kisiel, N.D., and Lee, L. 1994. Endogenous p53 protein generated from wild-type alternatively spliced p53 RNA in mouse epidermal cells. Mol. Cell. Biol. 14:1698-1708.

Medina, D., Kittrell, F.S., Lui, Y-J., Schwartz, M. 1993a. Morphological and functional properties of TM preneoplastic mammary outgrowth. Cancer Res. 53:663-667.

Medina, D., Kittrell, F.S., Osborn, C.J., Schwartz, M. 1993b. Growth factor dependence and gene expression in preneoplastic mouse mammary epithelial cells. Cancer Res. 53:668-674.

Reich, N.D., Oren, M., and Levine, A.J. 1883. Two distinct mechanisms regulate the levels of a cellular tumor antigen, p53. Mol. and Cell. Biol. 3:2143-2150.

Reich, N.C. and Levine, A.J. 1984. Growth regulation of a cellular tumour antigen, p53, in nontransformed cells. Nature. 308:199-201.

Wu, Y., Liu, Y., Lee L., Miner, Z., and Kulesz-Martin, M. 1994. Wild-type alternatively spliced p53: binding to DNA and interaction with the major p53 protein in vitro and in cells. EMBO. 13:4823-4830.

FIGURE 1: IMMUNOFLUORESCENCE IN TM3 CELLS

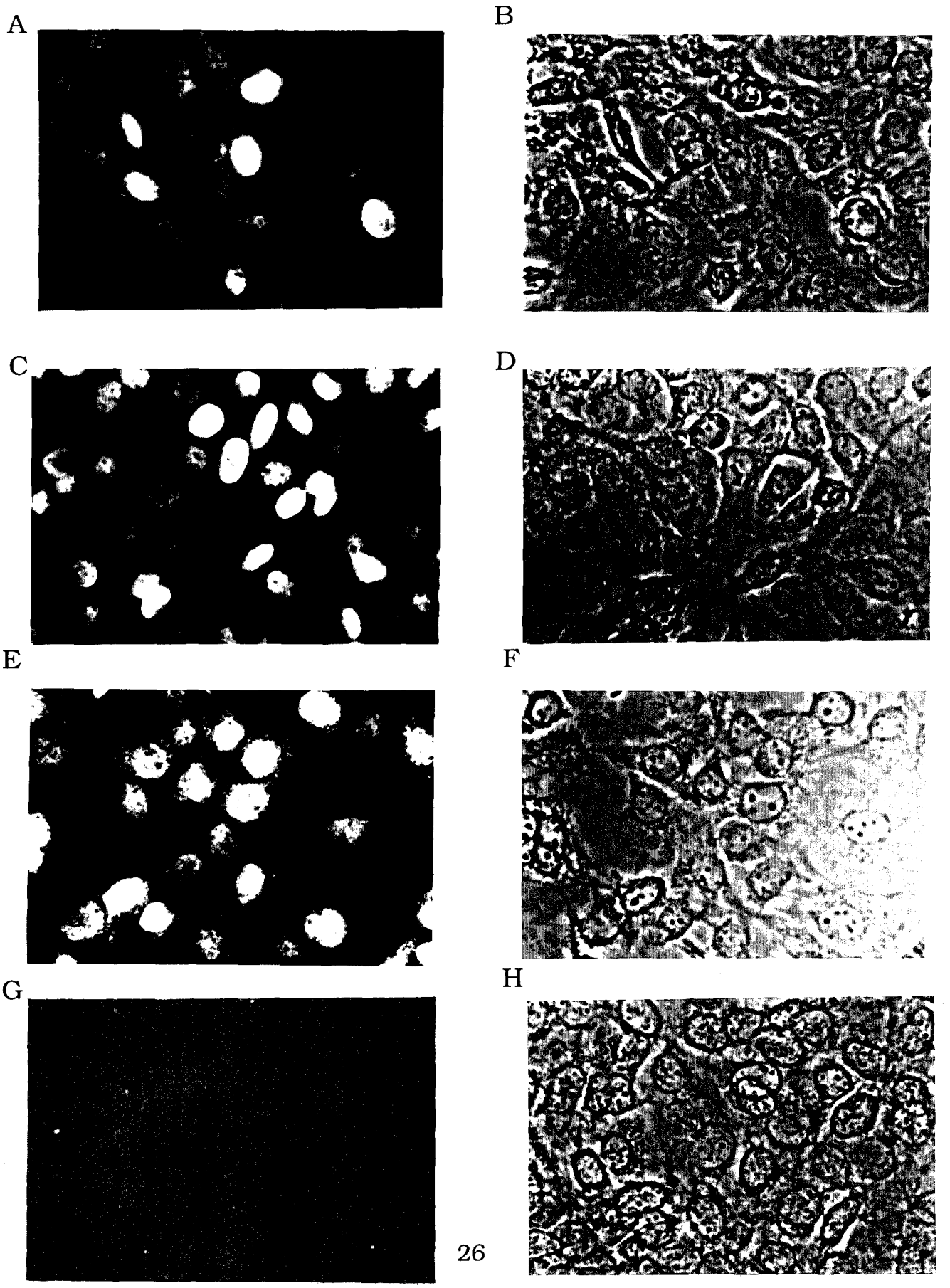

FIGURE 1: IMMUNOFLUORESCENCE IN TM10 CELLS

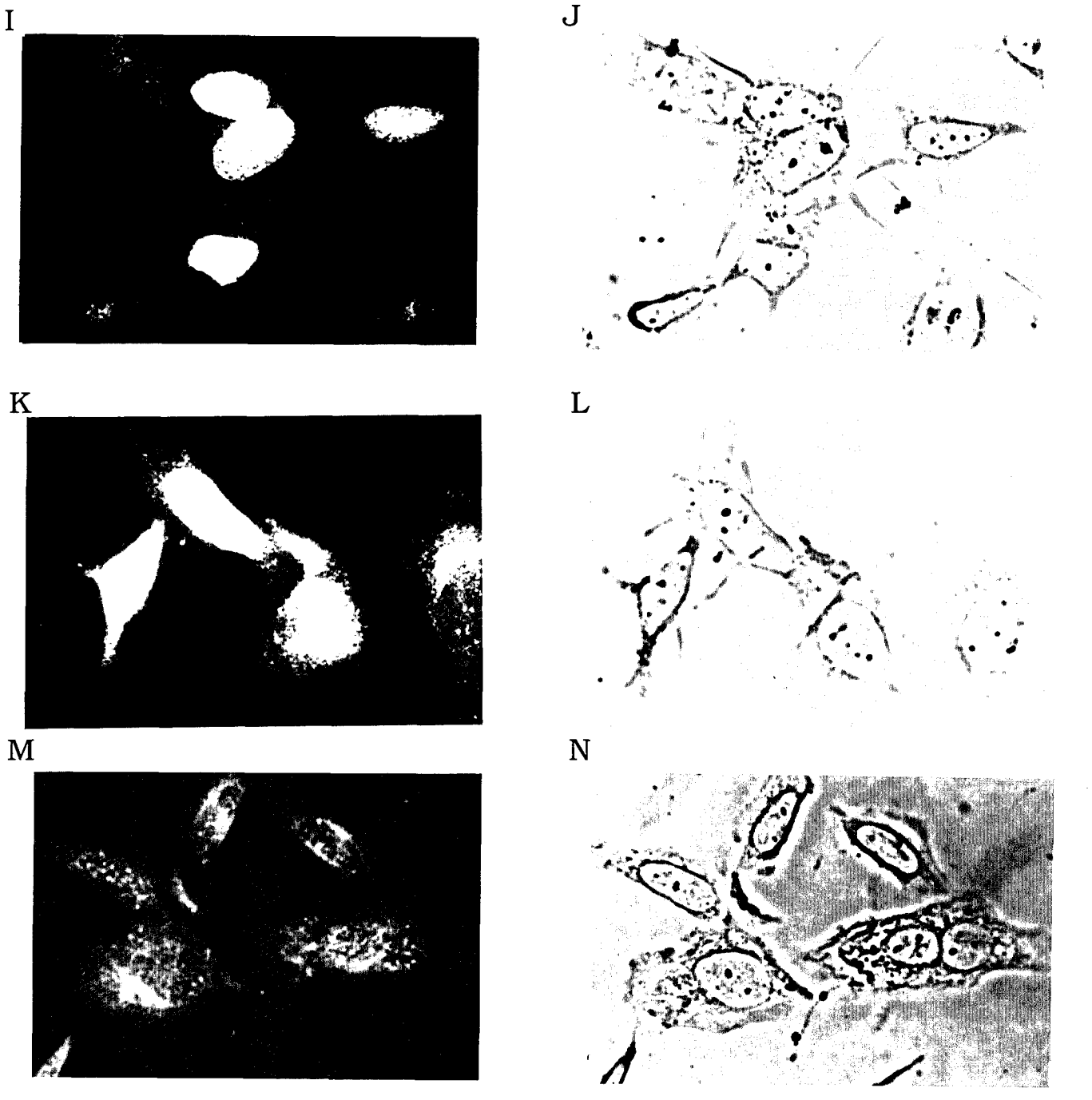

Figure 1. p53 and p53as antigen activity in TM3 and TM10 cells. Immunofluorescence fields of TM3 cells are shown in panels A, C, E, G, and for genistein treated TM10 cells in panels I, K, and M. Phase-contrast optics corresponding to the immunofluorescence fields are shown in panels B, D, F, H, J, L, and N. A, AsAp (Actinomycin D treated); C, PAb421; E, PAb240; G, Preimmune and IgG controls; I, ApAs; K, PAb421; M, Preimmune and IgG control. Untreated TM3 cells look similar to Actinomycin D treated cells when reacted with ApAs although the number of positive cells is less (see Table 2).

TABLE 1: REACTIVITIES OF ANTIBODIES AGAINST p53 PROTEINS

Ab	Wild type Conformation	Mutant Conformation	p53	p53as	Epitope
PAb421	+	+	+	-	370-378
PAb246	+	-	+	+	88-109
PAb 240	-	+	+	+	161-220
ApAs	+	+	-	+	(364-381)

All antibodies are mouse monoclonal antibodies commercially available from Oncogene Science, Inc. except ApAs which is a rabbit polyclonal specific for p53as made in this laboratory (Kulesz-Martin et al., 1994).

TABLE 2: IMMUNOFLUORESCENCE REACTIVITY OF p53 AND p53as ANTIBODIES TO TM CELL LINES

	ApAs	PAb421	PAb246	Pab240
TM3 untreated	8-29% 3^+ N	25% 3-4^+ N	neg	1-30% 3^+ N
TM3 ActD	31-43% 3^+ N	≥50% 3^+ N	neg	10-30% 3^+ N
TM4 untreated	50-95% 3-4^+ N	≥70% 3-4^+ N	neg	≥90% 2-4^+ N
TM4 ActD	50-95% 3-4^+ N	≥70% 3-4^+ N	neg	≥90% 2-4^+ N
TM12 untreated	neg	<0.1% 2-3^+ N	0.01-0.1% 2-3^+ N	neg
TM12 ActD	nd	nd	nd	nd
TM12 islands untreated	≤0.001% 3^+ N	≤0.01% 3-4^+ N	≥5% 3-4^+ N	neg
TM12 islands ActD	≤0.01% 3-4^+ N	≥0.01% 2-3^+ N	50-98% 3-4^+ N	neg
TM12 spaces untreated	neg	40% 2-4^+ N	40% 2-4^+ N	neg
TM12 spaces ActD	neg	40% 2-4^+ N	40% 3-4^+ N	neg
TM9 untreated	1-2% 2-4^+ N	≥50% 2-4^+ N	≥5% 3-4^+ N	≥60% 3-4^+ N

TABLE 2: IMMUNOFLUORESCENCE REACTIVITY OF p53 AND p53as ANTIBODIES TO TM CELL LINES

	ApAs	PAb421	PAb246	Pab240
TM10 untreated	≤0.001% 4^+ N	≤0.001% 4^+ N	≤0.001% 4^+ N	nd
TM10 ActD	≤0.1% 2.5^+ N	≤0.1% 4^+ N	≥0.01% 3^+ N	nd
TM10 Gen	20% $3\text{-}4^+$ N	≤0.01% 3^+ N	≤0.01% 3^+ N	nd
TM10 Xray	≤0.01% 3^+ N	≤0.01% $3\text{-}4^+$ N	≤0.01% $3\text{-}4^+$ N	

Percentages of cells reactive to each antibody are shown. Intensity of nuclear reactivity (N) was scored on a scale of 0 to 4^+. Actinomycin D (ActD) treatment was done at 0.5 nM, genestein treatment (Gen) was done at 60 nM, and X-ray treatment was done at 2000 rads. Actinomycin D treatments were carred out for 48 hours except for TM10 where all treatments were for 3 days. Neg = negative, nd = not done.

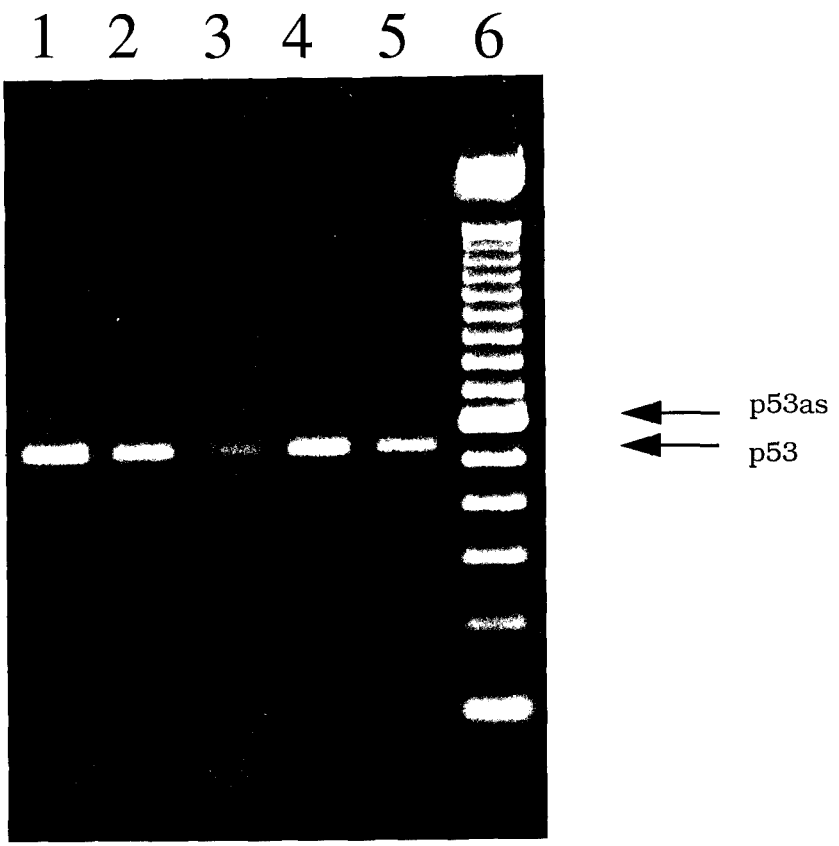

Figure 2. Agarose gel analysis of RT-PCR reactions from total RNA. Lane 1, TM3; Lane 2, TM4; Lane 3, TM12; Lane 4, TM12 islands; Lane 5, TM12 spaces; and Lane 6, molecular weight markers. The lower band (arrow) is approximately 517 basepairs derived from the regularly spliced p53, while the upper band (arrow) is approximately 613 basepairs and is derived from the alternatively spliced p53.

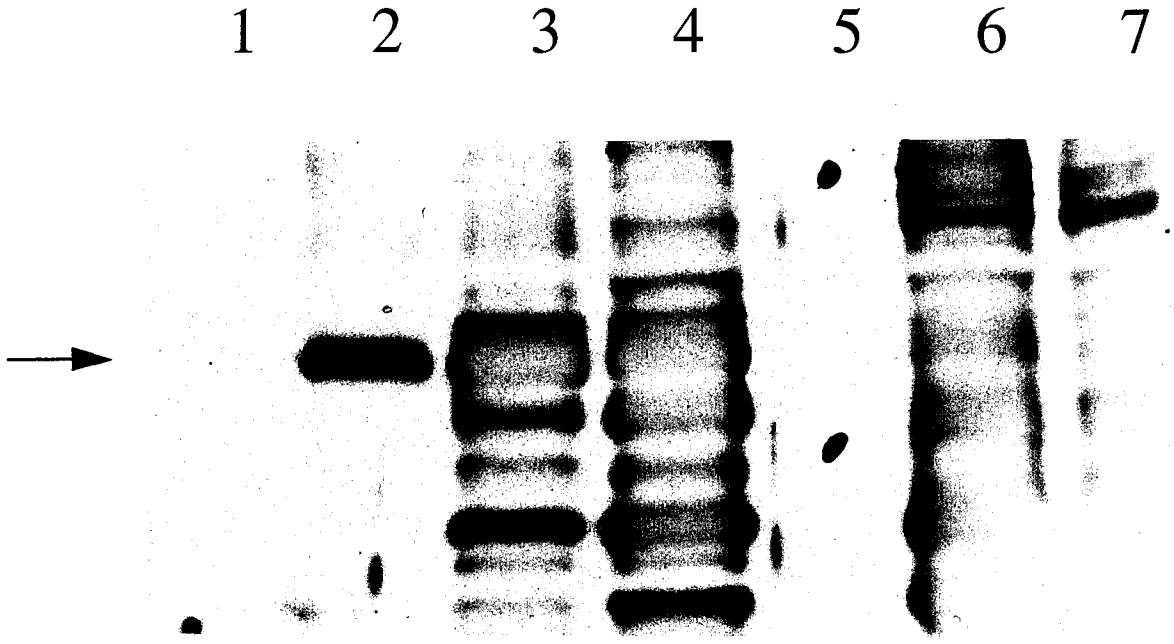

Figure 3. Western immunoblot analysis of the time course of p53as protein production following Sf9 infection by a p53as-recombinant baculovirus. Lane 1, immediately following infection; Lane 2, 1 day post infection; Lane 3, 2 days post infection; Lane 4, 3 days post infection; Lane 5, molecular weight marker; Lane 6, 4 days post infection; and Lane 7, 5 days post infection. Arrow indicates p53as protein. Western blotting utilized ApAs antibody.

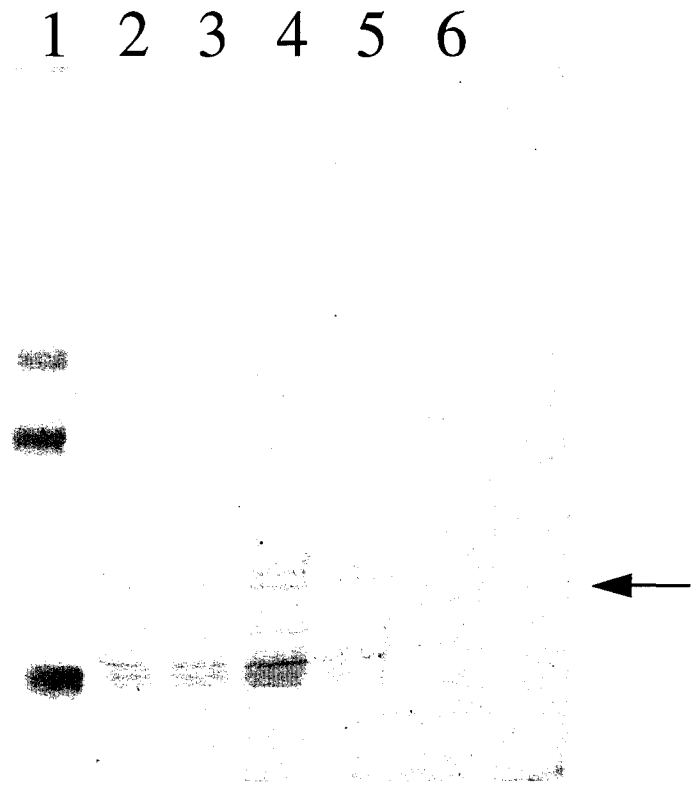

Figure 4. Coomassie Blue stained polyacrylamide gel analysis of PAb421 affinity column purification of human p53 protein. Lane 1, molecular weight markers; Lane 2, cleared lysate before column; Lane 3, flow through: Lane 4, wash; Lane 5, eluant 1; Lane 6, eluant 2. Equal amounts of protein were loaded in each lane. Arrow indicates the position of p53 protein.

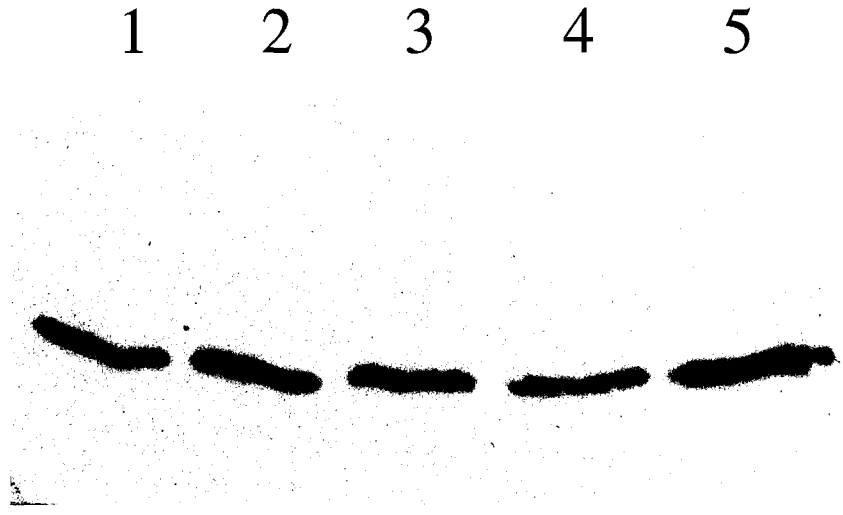

Figure 5. Western immunoblot analysis of PAb421 affinity column purification of human p53 protein. Lane 1, cleared lysate before column; Lane 2, flow through; Lane 3, wash; Lane 4, eluant 1; Lane 5, eluant 2. Equal amounts of protein were loaded in each lane. Western blotting utilized PAb421.

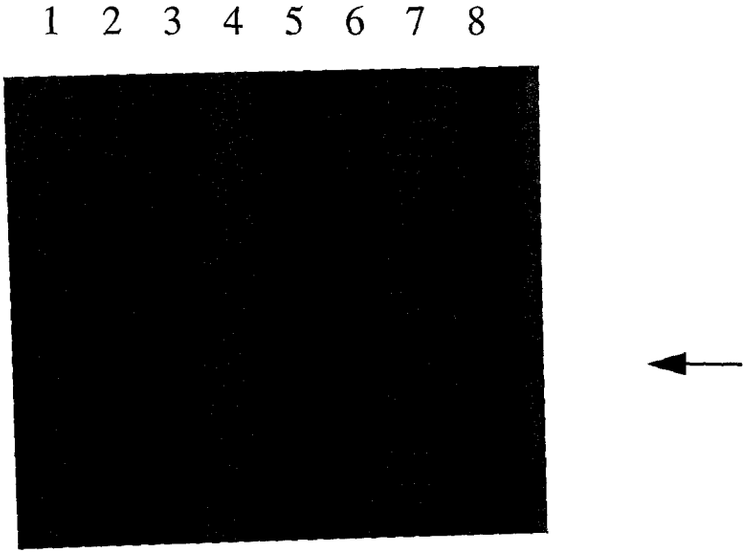

Figure 6. Coomassie Blue stained polyacrylamide gel analysis of PAb242 affinity column purification of mouse p53as protein. Lane 1, cleared lysate before column; Lane 2, flow through; Lane 3, wash 1; Lane 4, wash 2; Lane 5, wash 3; Lane 6 eluant before concentration; Lane 7, eluant after concentration; Lane 8, molecular weight marker. Equal amounts of protein were loaded in each lane. Arrow indicates the position of p53as protein.

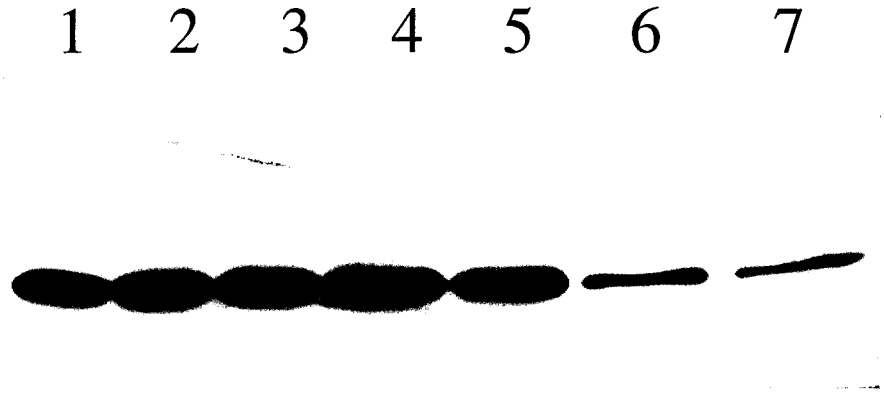

Figure 7. Western immunoblot analysis of PAb242 affinity column purification of mouse p53as protein. Lane 1, cleared lysate before column; Lane 2, flow through; Lane 3, wash 1; Lane 4, wash 2; Lane 5, wash 3; Lane 6, eluant before concentration; Lane 7, eluant after concentration. Equal amounts of protein were loaded in each lane. Western blotting utilized ApAs antibody.

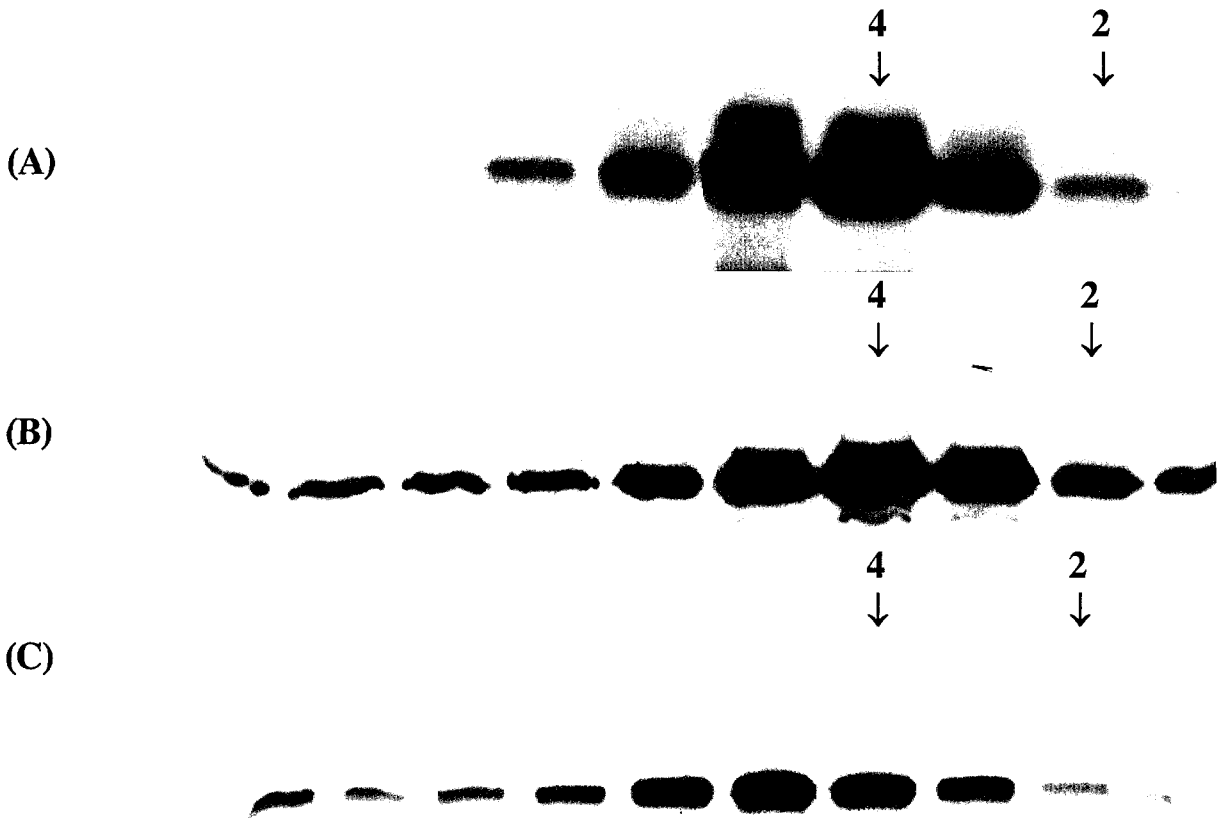

Figure 8. FPLC analysis of p53 and p53as proteins. (A) p53as, (B) p53, and (C) p53 + p53as. Proteins were translated in vitro. Arrows indicate the positions of tetramers (4) and dimers (2) based on molecular weight standards.

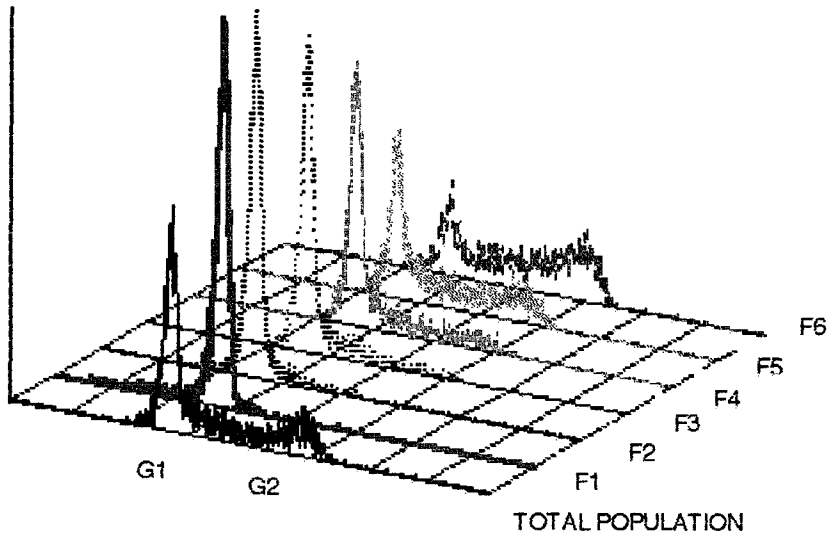

Figure 9. Centrifugal elutriation and flow cytometry of fixed TM3 cells. The first histogram on the overlay graph represents the beginning total population of TM3 cells. Subsequent histograms show the separation of cells based on DNA content of several fractions. Placement of G1 and G2 cell cycle stages on the x-axis was determined by using mouse spleen cells as an external control. Elutriated fractions (F) are indicated on the z-axis. Total population: G1, 53%; S, 23%; G2, 20%. Fraction 1: G1, 89%; S, 3%; G2, 0.4%. Fraction 6: G1, 25%; S, 34%; G2, 37%. Total cell numbers equal 100% with the remaining cells in these fractions predominantly >G2.

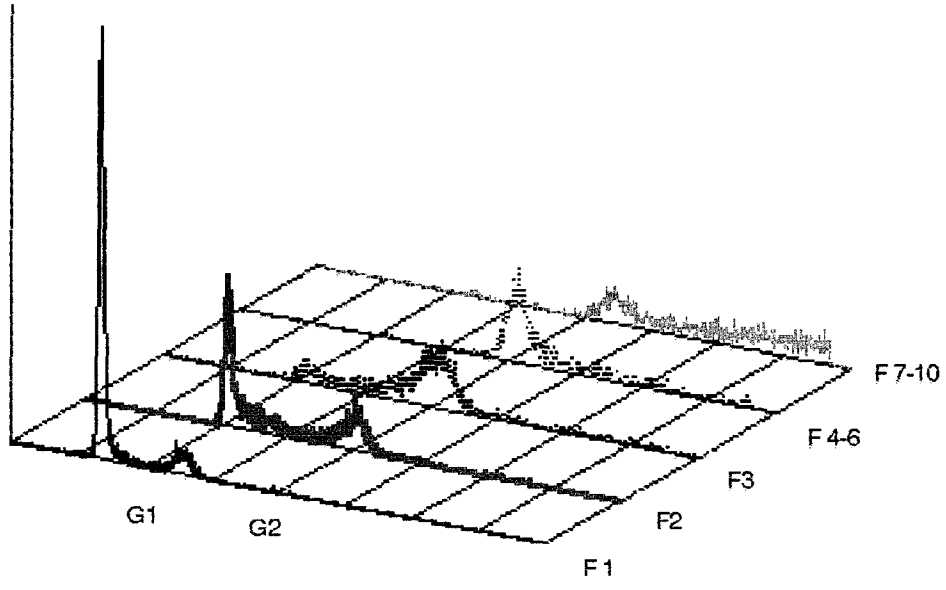

Figure 10. Centrifugal elutriation and flow cytometry of fresh TM4 cells. The histograms represent the DNA content of several elutriated fractions some of which were combined in preparation for cell sorting. Placement of G1 and G2 cell cycle stages on the x-axis was determined by using mouse spleencells as an external control. Occasional misalignment of a histogram due to technical difficulties was noted and is shown in this figure in fraction 1. Elutriated fractions (F) are indicated on the z-axis. Fraction 1: G1, 82%; S, 14%; G2, 3%. Fraction 2: G1, 40%; S, 17%; G2, 39%. Fraction 3: G1, 11%; S, 9%; G2, 68%. Fraction 4-6: G1, 2%; S, 1%; G2, 63%. Fractions 7-10: G1, 1%; S, 1%; G2, 25%. Total cell numbers equal 100% with the remaining cells in these fractions predominantly >G2.

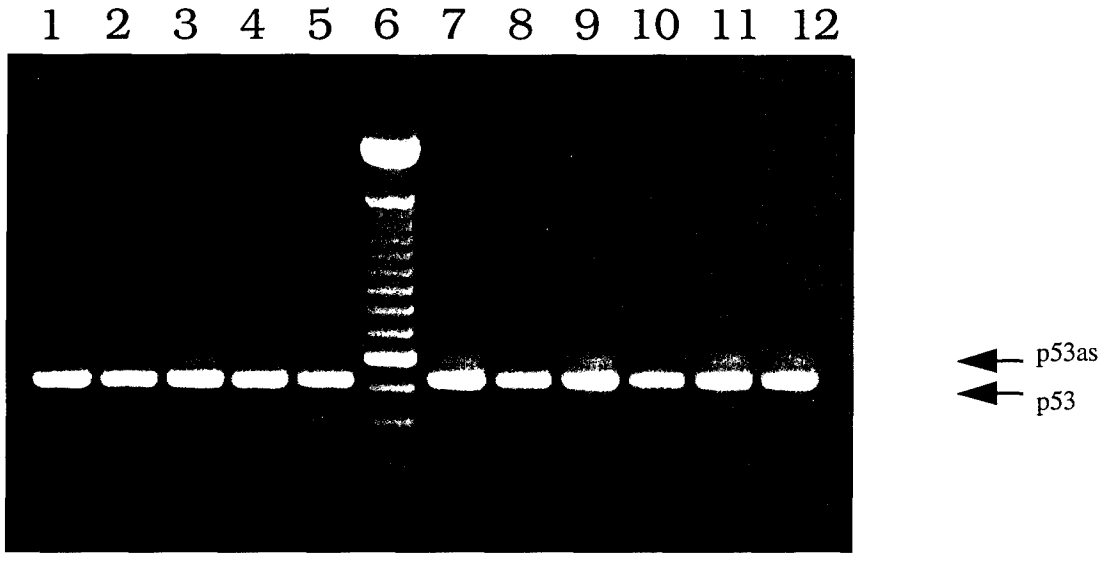

Figure 11. Agarose gel analysis of RT-PCR reactions from total RNA isolated from elutriated TM4 fractions. Lane 1, fraction 1 (G1); Lane 2, fraction 2 (G1): Lane 3, fraction 3 (G1/S); Lane 4, fraction 4 (G1/S); Lane 5, fraction 5 (S/G2); Lane 6, molecular weight marker; Lane 7, fraction 6 (S/G2); Lane 8, fraction 7 (G2); Lane 9, fraction 8 (>G2); Lane 10, fraction 9 (>G2), Lane 11, fraction 10 (>G2); Lane 12, beginning total cell population. The lower band (arrow) is approximately 517 basepairs derived from the regularly spliced p53, while the upper band (arrow) is approximately 613 basepairs and is derived from the alternatively spliced p53.

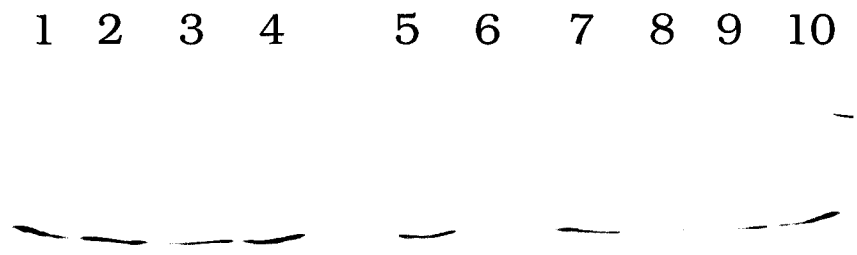

Figure 12. Western blot analysis of cell lysates from elutriated TM4 fractions. Lane 1, fraction 2 (G1); Lane 2, fraction 3 (G1/S): Lane 3, fraction 4 (G1/S); Lane 4, fraction 5 (S/G2); Lane 5, fraction 6 (S/G2); Lane 6, fraction 7 (G2); Lane 7, fraction 8 (>G2); Lane 8, fraction 9 (>G2); Lane 9, fraction 10 (>G2); Lane 10, beginning total cell population. Equal amounts of protein were loaded in each lane. Western blotting utilized PAb421.

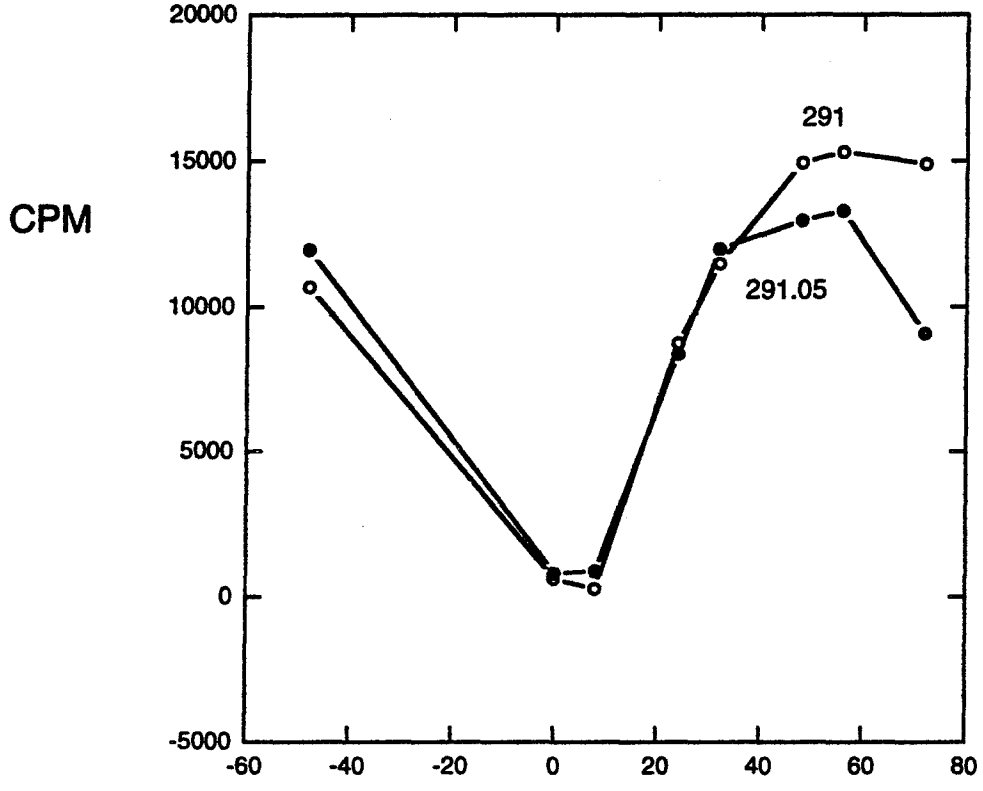

Figure 13. Tritiated thymidine uptake into DNA after release of growth arrest in cells that were serum starved. Open circles, 291 cells; closed circles, 291.05RAT cells.

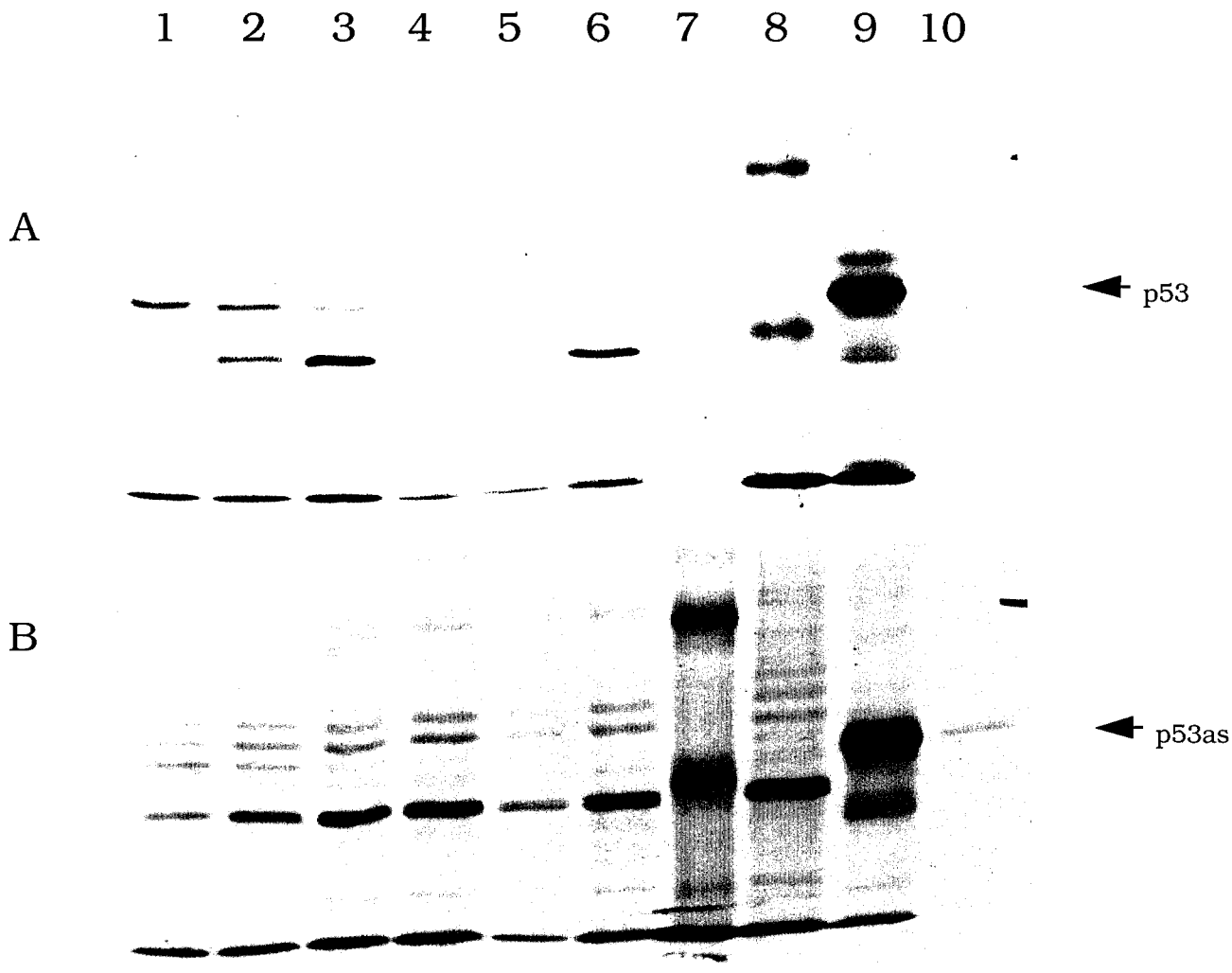

Figure 14. p53 and p53as half life determination in asynchronous proliferating TM3 cells. Immunoprecipitation analysis at several chase time points. A) Precipitating antibody, PAb421. Lane 1, 0 hour post chase; Lane 2, 2 hours post chase; Lane 3, 4 hours post chase; Lane 4, 6 hours post chase; Lane 5, 8 hours post chase; Lane 6, 10 hours post chase; Lane 7, IgG2A control using the 0 time point lysate; Lane 8, molecular weight marker; Lane 9, in vitro translated p53; Lane 10, IgG2A control for in vitro translated protein. Arrow indicates p53 protein position. B) Precipitating antibody, ApAs. Lane 1, 0 hour post chase; Lane 2, 2 hours post chase; Lane 3, 4 hours post chase; Lane 4, 6 hours post chase; Lane 5, 8 hours post chase; Lane 6, 10 hours post chase; Lane 7, molecular weight marker; Lane 8, preimmune control using the 0 time point lysate; Lane 9, in vitro translated p53as; Lane 10, preimmune control for in vitro translated protein. Arrow indicates p53as protein position.

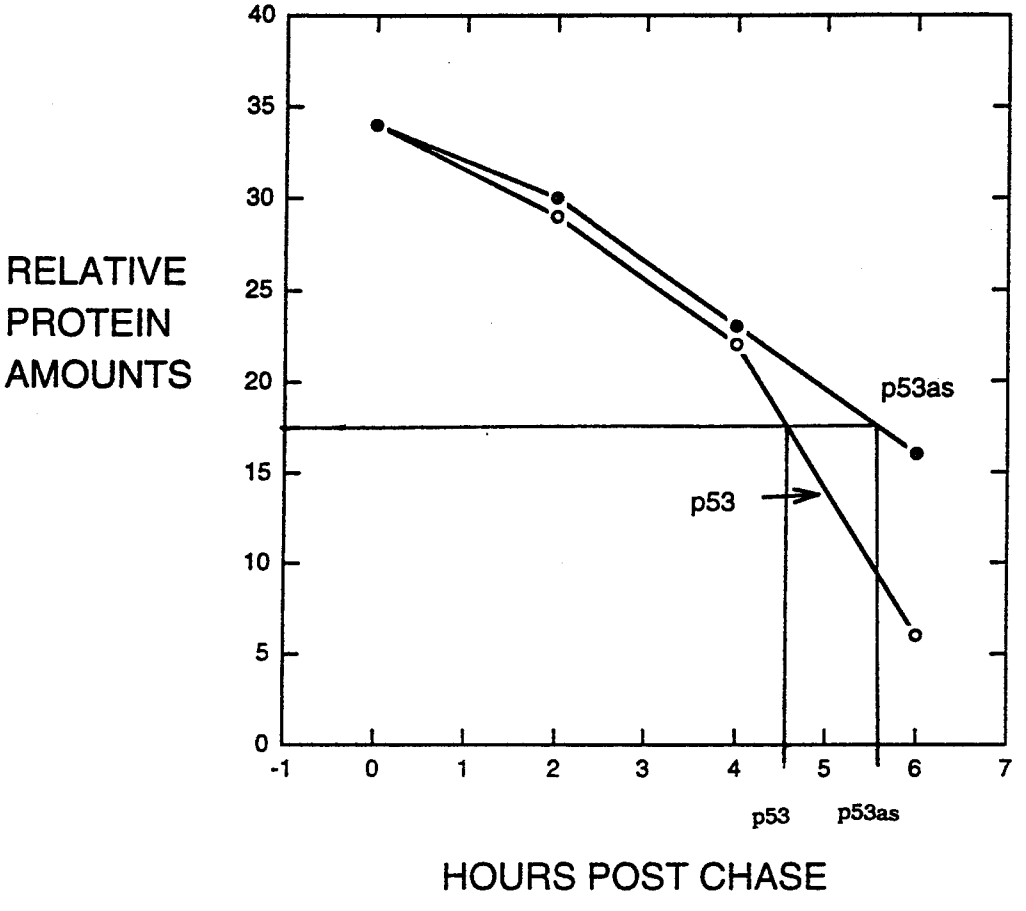

Figure 15. Determination of half life of asynchronous proliferative TM3 cells utilizing densitometric scanning analysis of Figure 14. Open circles, p53; closed circles, p53as. Half life of each protein is indicated on the graph.

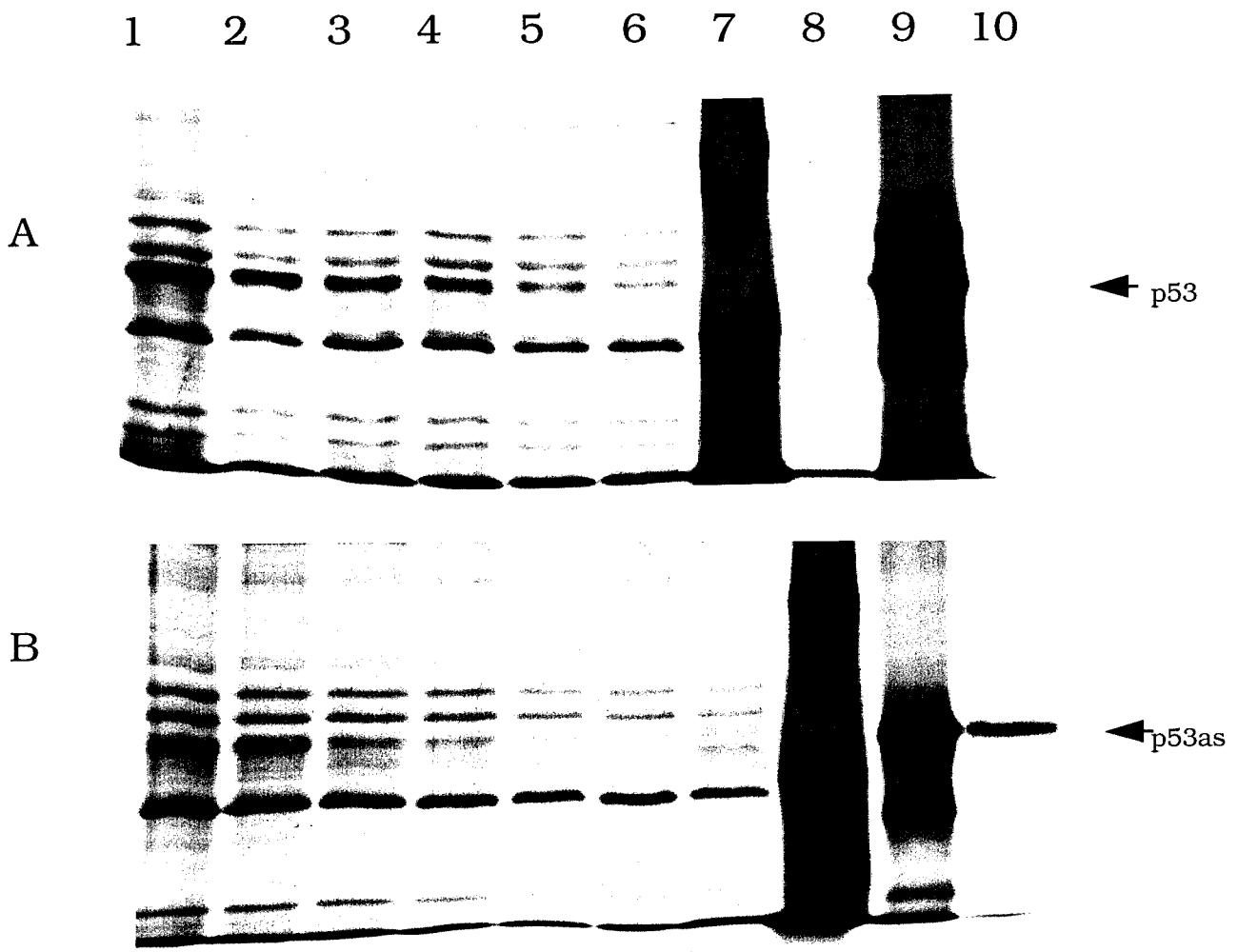

Figure 16. p53 and p53as half life determination in asynchronous proliferating TM4 cells. Immunoprecipitation analysis at several chase time points. A) Precipitating antibody, PAb421. Lane 1, 0 hour post chase; Lane 2, 2 hours post chase; Lane 3, 4 hours post chase; Lane 4, 6 hours post chase; Lane 5, 8 hours post chase; Lane 6, 10 hours post chase; Lane 7, molecular weight marker Lane 8, IgG2A control using the 0 time point lysate;; Lane 9, in vitro translated p53; Lane 10, IgG2A control for in vitro translated protein. Arrow indicates p53 protein position. B) Precipitating antibody, ApAs. Lane 1, 0 hour post chase; Lane 2, 2 hours post chase; Lane 3, 4 hours post chase; Lane 4, 6 hours post chase; Lane 5, 8 hours post chase; Lane 6, 10 hours post chase; Lane 7, preimmune control using the 0 time point lysate; Lane 8, molecular weight marker; Lane 9, in vitro translated p53as; Lane 10, preimmune control for in vitro translated protein. Arrow indicates p53as protein position.

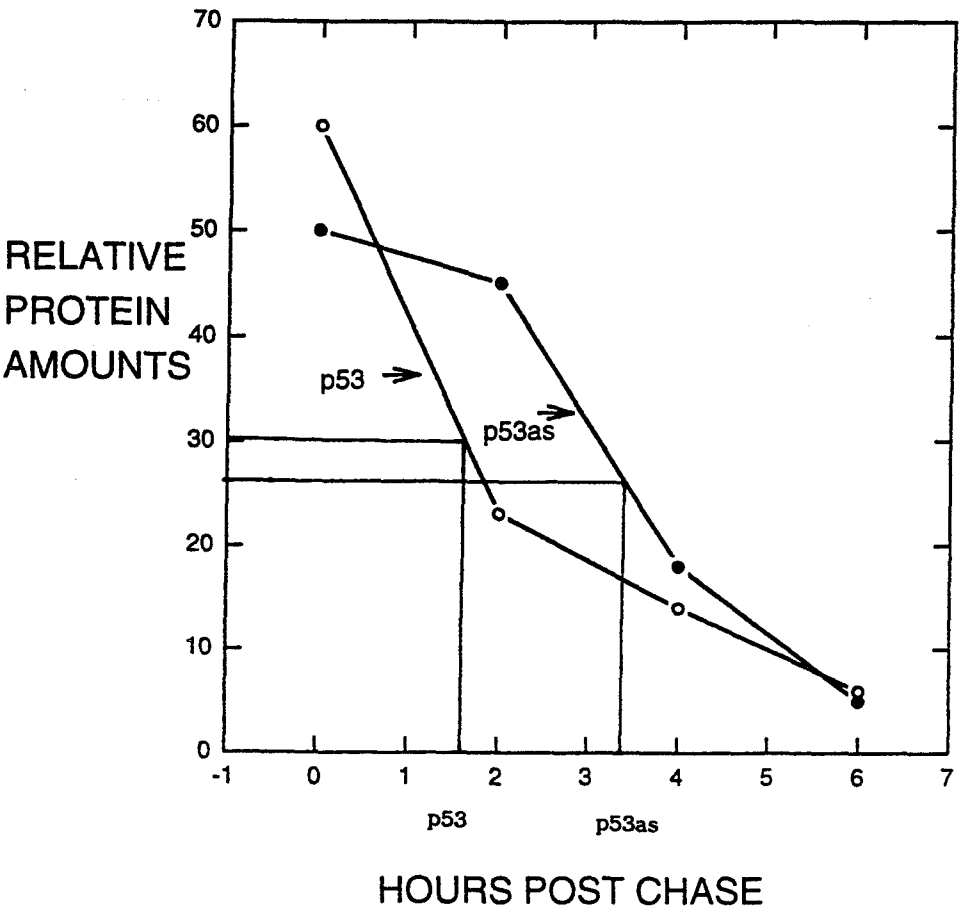

Figure 17. Determination of half life of asynchronous proliferating TM4 cells utilizing densitometric scanning analysis of Figure 16. Open circles, p53; closed circles, p53as. Half life of each protein is indicated on the graph.